Revealing How Interactions Lead to Ordering in *Para*-Terphenyl

D. J. Goossens*
Research School of Chemistry and Department of Physics, Australian National University, Canberra, ACT 0200, Australia
M. J. Gutmann
ISIS Facility, Rutherford Appleton Laboratory, Chilton, Didcot, Oxon, United Kingdom
(Received 19 October 2008; published 9 January 2009)

How does the ordering in a crystal arise from the interactions present? Crystal structure determination shows what the crystal structure is, but in solving directly for atomic coordinates leaves questions as to why (or how) aspects of the structure arise. The answers to such questions are crucial in the study of what drives structural phase transitions or in crystal structure prediction. In this work, modeling of the neutron diffuse scattering from deuterated *para*-terphenyl, $C_{18}D_{14}$, shows directly how the observed short-range order arises out of intramolecular and intermolecular interactions. This approach provides real-space descriptions of cooperative molecular motions and correlations, and explains the two-dimensional critical behavior observed in other experiments. In doing so, it is found that intramolecular and intermolecular interactions, and the molecules themselves, can be thought of as acting as nanoscale mechanical linkages.

DOI: 10.1103/PhysRevLett.102.015505 PACS numbers: 61.05.fg, 05.10.Ln, 78.40.Pg

Introduction.—Diffuse scattering from a crystalline material is the coherent scattered intensity in a diffraction pattern that is not localized on the reciprocal lattice points. It comes about due to short-range order (SRO) in the crystal and is sensitive to two-body correlations. Its analysis can determine details about the nature of the SRO in the crystal [1]. Here, we use analysis of diffuse scattering to show how the SRO arises from basic intramolecular and intermolecular interactions. We model SRO via modeling the interactions in the system rather than through direct solution for atomic or molecular coordinates. Such modeling lends itself to examining how the observed ordering grows out of the interactions.

Para-terphenyl (ptp) undergoes a structural phase transition at 193 K, deuterated *para*-terpheny (d-ptp) at $T_C \sim 178$ K [2]. The high temperature phase is monoclinic with lattice parameters $a = 8.106(4)$ Å, $b = 5.613(2)$ Å, $c = 13.613(6)$ Å, and $\beta = 92.04(4)°$ (spacegroup $P2_1/a$) [3].

Figure 1 shows a molecule of ptp. There are conflicting interactions within the molecule—the interring H-H contacts between orthohydrogens (dashed line) which are too short when the molecule is ''flat'' force the adjacent rings to be noncoplanar while the conjugation of the π orbitals on the phenyl rings prefers a coplanar arrangement for all rings. The result is that the central ring of each molecule lies at an angle to the plane containing the outer rings, with two possible senses of twist. Below T_C, these twists order in a long-ranged fashion, with the sign of the twist alternating along both a and b, giving a doubled $P1$ cell [4,5]. Above T_C, the range of this ordering is finite so that the average molecule is a 50:50 superposition of twists of both senses, with the two senses apparent in the atomic displacement parameters. The double-peaked distribution of the torsional angle on the central phenyl ring as derived from Bragg studies is presented in the literature [6,7]. The key parameters are the separation of the histogram maxima ($\sim 26°$) and the histogram value at zero twist, which is an indicator of barrier height. The distribution thus derived has been compared to results from molecular dynamics simulation [8]. That work takes some account of intermolecular correlation, but is limited by the small size of detailed molecular dynamics simulation—$4 \times 4 \times 2$ unit cells. Such a simulation is too small to Fourier transform when modeling the diffuse scattering because correlations that give rise to the scattering extend over many unit cells [9].

Diffuse scattering in para-terphenyl.—Figure 2 shows two cuts through the three-dimensional diffuse scattering pattern of a single crystal of d-ptp, as measured at 200 K using neutron diffraction on the single crystal diffracometer, SXD, at ISIS [10]. Patterns were also collected at room temperature and at 70 K. Figure 2(a) shows the $hk0$ plane of reciprocal space while Fig. 2(b) shows the $h0.5l$

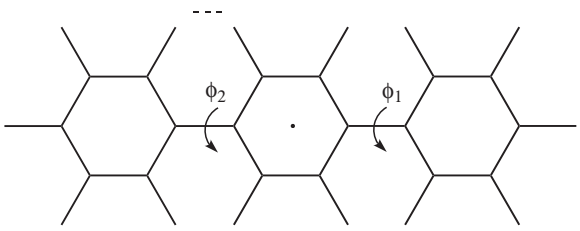

FIG. 1. Schematic diagram of a molecule of *para*-terphenyl. ϕ_i indicates an internal degree of freedom while the dashed line shows an example of the intramolecular interactions that force the molecule away from planarity. In practice only one angle is used—the angle of the center phenyl ring to a plane containing the outer rings.

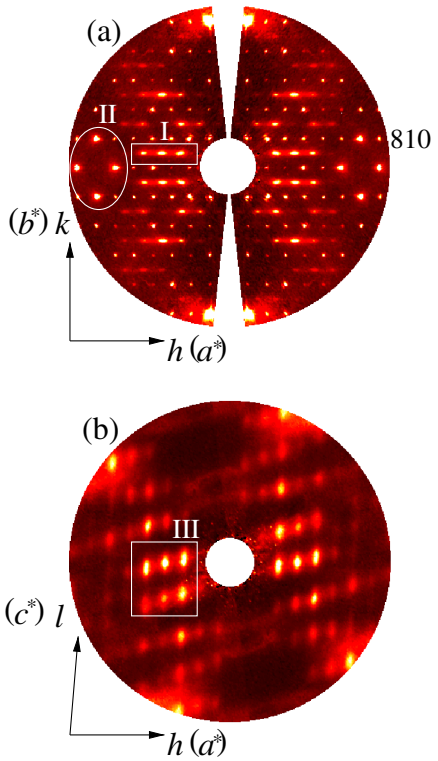

FIG. 2 (color online). Two slices of diffuse scattering data. (a) The $hk0$ (a^*b^*) plane and (b) the $h0.5l$ plane. Highlighted features are discussed in the text. The images are color maps in which white is maximum intensity and black is zero (or regions not accessed in the experiment). (a) Contains Bragg peaks which are truncated.

plane. The oblong peaks inside rectangle I (and III) are examples of peaks due to the SRO in the twists on the d-ptp molecules. The features in box II are due to correlations in the displacive motions of the adjacent molecules. Of most interest here is I. The large oval regions of diffuse scattering at the $(hkl) + (\pm 1/2 \pm 1/2\, 0)$ Bragg positions are incipient Bragg peaks, and below T_C they sharpen into real Bragg peaks. These show that the twists alternate in sign over the short range, as was already known [9]. The strong anisotropy indicates that the correlations are much stronger in the b direction than in the a direction. There is no apparent correlation along c, as expected, since it is the outer phenyl groups that contact from molecule to molecule in this direction, so molecules stacked along c are essentially insulated from the occupancies on their neighbors. Figure 2(b) shows the $h0.5l$ cut. Box III contains the same spots as box I in Fig. 2(a), but viewed down b^* rather than c^*.

Modeling.—Inspection of the average crystal structure suggests a mechanism whereby the molecules might be linked such that the twists will correlate as the data suggest. Figure 3 shows the key contact vectors that propagate the torsional twists (only those connecting inner rings with inner rings are shown). Consider molecules A and B—

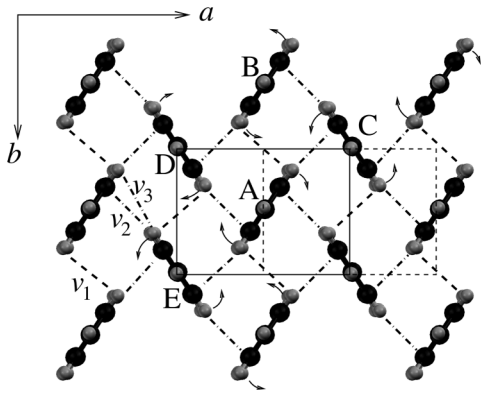

FIG. 3. The key contacts in propagating the occupancy correlations, viewed down the long axis of the molecules; molecules drawn as "flat." Arrows illustrate the cooperative motions of the central phenyl rings on neighboring molecules. The rectangles (solid lines and dashed lines) show opposite ab faces of the unit cell (the long molecular axis is not parallel to c). Small gray spheres are H (D), large black ones are C. Labels A, B, etc. are referred to in the text.

these are nearest neighbors along b, and it is quite clear that the contact vectors represented by dashed lines (for example v_1) will give rise to a negative correlation between rotations on A and B. (Center phenyl ring rotations are noted by curved arrows.) This is a direct interaction, hence the strong correlation in the twists along b [b^* (k) is the direction in which the diffuse spots in box I of Fig. 2 are narrow]. The mechanism for propagating the twists along a is subtle. As molecule A rotates as noted, the dot-dashed lines contact with atom C (type v_2) will cause C to rotate as shown. The dot-dashed line contact from A to D might be expected to make D rotate in the same sense as C, but note that as the contacting atom on A gets closer to D, D can maintain the atom-atom distance by rotation in *either* sense. It is the indirect interaction of A with D via E that "chooses" the direction of rotation of D. So D rotates oppositely to C, but the correlation is weak as the interaction is indirect. The final correlation structure is inherently the result of cooperative ab-plane motions of the assembly of molecules—molecular scale rods and levers.

This model was tested in the following manner: A model crystal of $32 \times 32 \times 32$ unit cells was constructed in which the molecules were placed on their average positions. A torsional potential of the form

$$E_{\mathrm{tor}} = F_{\mathrm{tor}} \phi^2_{\mathrm{c.r.}} \tag{1}$$

was placed on the twist angle of the central phenyl ring. Here F_{tor} is a force constant, $\phi_{\mathrm{c.r.}}$ is the angle of the center ring relative to the plane of the outer rings, and E_{tor} is the energy cost of twisting that ring. This acts to keep the molecule flat and is a simple model for the interaction of the π orbitals on the phenyl rings. The interatomic distance noted by the dashed line in Fig. 1 is too short if the molecule is flat (it is ~2 Å and a H-H contact distance

should be at least 2.4 Å) and this energy will be reduced if the molecule is not flat. It is modeled by a simple quadratic dependence

$$E_{\text{H-H}} = F_{\text{H-H}} \sum_{\text{H-H pairs}} (d - d_0)^2, \qquad (2)$$

where $F_{\text{H-H}}$ is a force constant, d_0 is the "ideal" H-H distance, and H-H is the resulting energy contribution when summing over all H-H pairs. $E_{\text{H-H}} + E_{\text{tor}} = E_{\text{intra}}$, the intramolecular energy, and correct choice of F_{tor} relative to $F_{\text{H-H}}$ will give a double-well potential such that the distribution of molecular twists will approximate that deduced from Bragg scattering studies—however, this takes no account of the role of intermolecular interactions.

To induce SRO there must be intermolecular interactions. These use a form like Eq. (2) but connect neighboring molecules. Initially the molecules were held fixed at their origins, and the orientations of the outer phenyl rings were fixed. The only molecular motion was rotation of the central ring, like a molecular seesaw. Molecules interacted via contact vectors between central phenyl rings (Fig. 3). The vector equilibrium lengths were taken from the interatomic distances for equivalent atoms on the outer rings, as these are a good measure of the preferred separation of rings that are not subject to twists. Summing over the interactions connecting a molecule to its neighbors gives an intermolecular energy, E_{inter}, and $E_{\text{inter}} + E_{\text{intra}} = E_{\text{mol}}$, the molecular energy. By using a simple Monte Carlo algorithm, the twists on molecules were made to interact, and a correlation structure was formed. The Monte Carlo algorithm was as follows: (1) A molecule was randomly selected from the array of unit cells, (2) its energy was calculated as outlined above, (3) its torsional angle was randomly modified by some small amount, (4) its energy was recalculated, (5) the new configuration was accepted or rejected according to a Metropolis algorithm [11].

By on average visiting each molecule several thousand times, correlations between the twists on adjacent molecules were induced. Hence a good model inherently shows how the SRO arises out of the interactions (even if these interactions are modeled very simply). Interactive optimization of such a simple "seesaw" model could well reproduce the scattering in box I of Fig. 2(a), but allowing the molecular centers of mass to shift, and allowing the molecules as a whole to reorient, was necessary to produce the diffuse features of displacive origin (box II in Fig. 2). This required the outer rings on adjacent molecules to interact to act as a framework within which the inner-ring interactions operate on adjacent twists. Contact vectors along the c axis were needed to cause an extra modulation apparent in the $h0.5l$ plane such that the elongated spots boxed in Fig. 2(b) were split into pairs as observed, rather than forming a single large streak.

Final model.—The diffraction patterns calculated from the final model are shown in Fig. 4. There were found to be six key parameters: (F_{tor}, $F_{\text{H-H}}$, three F_i, and one parameter used to modify the equilibrium lengths of contact vectors v_2 and v_3 (Fig. 3) such that d_{0v_3} is 0.3 Å longer in this model than in the simpler one discussed above, and d_{0v_2} is 0.3 Å shorter. (The actual changes in average length of v_2 and v_3 were minor ~ -0.03 Å and $\sim +0.01$ Å, respectively.) F_1 is the force constant between inner rings and which acts in the ab plane (this is the force constant on vectors v_1, v_2, and v_3 shown in Fig. 3). F_2 is the force constant on the outer rings in the ab plane (equivalent to v_1, v_2, and v_3), and F_3 connects molecules along a direction parallel with their long axes. The diffraction patterns shown in Fig. 4 have these force constants in the ratios F_{tor}:$F_{\text{H-H}}$:F_1:F_2:F_3 = 4.62:6.25:1:2:1, with $F_1 = F_3 = 2.3 \pm 0.2 k_B T$ Å^{-1}. Given the great simplicity of the model, the agreement is remarkable.

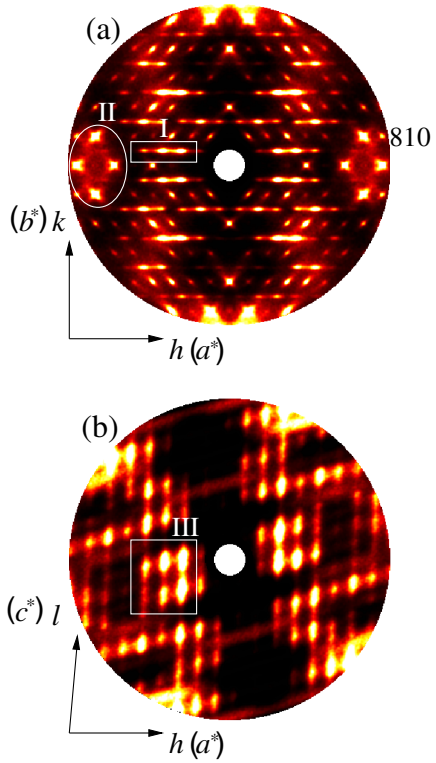

FIG. 4 (color online). The diffuse scattering in the (a) $hk0$ (a^*b^*) plane and (b) $h0.5l$ plane of reciprocal space calculated from the final model.

Figure 5 shows the histogram of center-ring twist angles from the final model presented here and from the literature [6,7]. Most likely due to the simplified forms for the potentials, the agreement is not perfect—in particular, the model presented here shows the minima separation to be ~37° where fitting to diffraction data suggests 26° [6]. However, the minima width is well reproduced, as is the histogram value at zero twist, suggesting that the barrier height is also appropriate.

The potentials are harmonic so the model does not capture the structural phase transition. It does show the

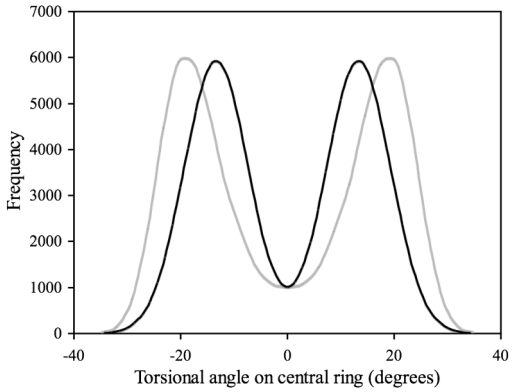

FIG. 5. The histogram of center-ring twist angles from the final model presented here (gray line) and from the literature (black line) [6,7]. Data have been normalized by the number of molecules in the simulation.

key mode; as temperature falls and the correlation lengths along a and b diverge, the cooperative motions must lock in and the phase transition occurs. The isolation of the central phenyl rings results in the correlated regions being essentially two dimensional, giving two-dimensional critical fluctuations that were inferred previously [12], but which here arise naturally from the correlating mechanism.

Conclusions.—This Letter shows that we can use the analysis of diffuse scattering to build up a real-space picture of how molecular interactions lead to molecular ordering. The main significance of the work lies in its ability to provide new information in studies of important materials. For example, the development of a real-space picture of the key mode in the structural phase transition readily explains the measured critical behavior. Identifying key intermolecular interactions shows which sites on the molecules might best be chemically altered to modify their physical properties.

The relationships between intermolecular and intramolecular interactions and the resulting crystal structure in molecules such as ptp are important because of the ability to use chemistry and particularly pressure [13–15] to tune the structure and therefore the properties, which have been shown to be very sensitive to the details of the three-dimensional structure (and therefore to how the structure arises) [16]. The work presented here adds to these studies because by looking at the SRO we see *how* the molecular conformations adjust in order to accommodate each other. This feeds into information about the real intermolecular distances and how they are different from those apparent in conventional crystallographic studies, and how they will behave when pressure is applied. This in turn must be taken into account in any detailed modeling such as density functional approaches [15,16]. Similarly, SRO studies indicate what the population of local configurations is, which can also be fed into, or act as a test of, computational modeling. It also shows that the molecules are highly unlikely to be "flat" in ptp. Some work assumes rigid flat molecules [15], yet any calculations that use intermolecular distances based on such a model are perforce limited.

We gratefully acknowledge the Australian Institute for Nuclear Science and Engineering, the Australian Partnership for Advanced Computing, and the Access to Major Research Facilities Program for financial support. We thank Dr. R. O. Piltz of ANSTO for work in sample characterization.

*Also at Department of Physics, Australian National University, Canberra, ACT 0200, Australia.
goossens@rsc.anu.edu.au

[1] T. R. Welberry, *Diffuse X-Ray Scattering and Models of Disorder*, IUCr Monographs on Crystallography (Oxford University Press, Oxford, 2004).
[2] R. E. Lechner, B. Toudic, and H. Cailleau, J. Phys. C **17**, 405 (1984).
[3] H. M. Rietveld, E. N. Maslen, and C. J. B. Clews, Acta Crystallogr. Sect. B **26**, 693 (1970).
[4] P. J.-L. Baudour, Y. Délugeard, and H. Cailleau, Acta Crystallogr. Sect. B **32**, 150 (1976).
[5] P. J.-L. Baudour and G.-P. Charbonneau, Acta Crystallogr. Sect. B **30**, 1379 (1974).
[6] P. J.-L. Baudour, H. Cailleau, and W. B. Yelon, Acta Crystallogr. Sect. B **33**, 1773 (1977).
[7] P. J.-L. Baudour, Acta Crystallogr. Sect. B **47**, 935 (1991).
[8] P. Bordat and R. Brown, Chem. Phys. **246**, 323 (1999).
[9] T. R. Welberry and S. L. Mair, J. Phys. C **20**, 4773 (1987).
[10] D. A. Keen, M. J. Gutmann, and C. C. Wilson, J. Appl. Crystallogr. **39**, 714 (2006).
[11] N. Metropolis, A. W. Rosenbluth, M. N. Rosenbluth, A. H. Teller, and E. Teller, J. Chem. Phys. **21**, 1087 (1953).
[12] T. Gullion, M. S. Conradi, and A. Rigamonti, Phys. Rev. B **31**, 4388 (1985).
[13] K. Hummer, P. Puschnig, and C. Ambrosch-Draxl, Phys. Rev. B **67**, 184105 (2003).
[14] G. Heimel, P. Puschnig, M. Oehzelt, K. Hummer, B. Koppelhuber-Bitschnau, F. Porsch, C. Ambrosch-Draxl, and R. Resel, J. Phys. Condens. Matter **15**, 3375 (2003).
[15] P. Puschnig, K. Hummer, C. Ambrosch-Draxl, G. Heimel, M. Oehzelt, and R. Resel, Phys. Rev. B **67**, 235321 (2003).
[16] A. Ferretti, A. Ruini, E. Molinari, and M. J. Caldas, Phys. Rev. Lett. **90**, 086401 (2003).